STUDY OF TWO GALACTIC CENTER STAR-FORMING REGIONS: SGR B AND SGR C

C. Law, F. Yusef-Zadeh
Northwestern University
Evanston, IL, 60208, U.S.A.
CLAW@NORTHWESTERN.EDU, ZADEH@NORTHWESTERN.EDU

Abstract

A variety of observations have shown Sgr B (G0.6−0.1) to be one of the most spectacular star-forming regions in the Galaxy. Similarly, Sgr C (G359.4−0.1) is host to sites of star formation as well as a collection of unusual non-thermal radio filaments. Using *Chandra*, Very Large Array, and Nobeyama Radio Observatory observations, we study the correlations between radio continuum, CS(1–0) molecular line, and X-ray emission from these sources, with a focus on the distribution of the neutral iron 6.4 keV line emission. We examine the hypothesis that such emission is evidence of past flaring from Sgr A* and present an alternative model. We also study the distribution of X-ray and radio point sources throughout these regions.

1 Introduction: Sgr B and Sgr C

Sgr B and Sgr C are molecular H II complexes known to be host to massive star formation. Each has clear signs of current star formation in the form of masers and compact H II regions.

The molecular clouds from which these stars are forming are also luminous in hard X-rays. One spectral line in particular, the 6.4 keV neutral iron fluorescence line, has been observed from Sgr B and Sgr C (Murakami et al., 2000).

Sgr B is characterized by

- prolific maser activity (Mehringer & Menten, 1997)
- over 30 compact H II regions powered by stars of type B0 or earlier (Mehringer et al., 1993)
- unusual molecular line kinematics, possibly indicating a recent collision between molecular clouds (Sato et al., 2000)
- a high mass of $\sim 10^7\ M_\odot$ (Mehringer et al., 1993).
- extreme column densities, $N_{\rm H} \sim 10^{24}$ cm^{-2} toward embedded stellar sources (Mehringer et al., 1993)

Sgr C is characterized by

- bright non-thermal radio filaments; these curious objects are often found associated with star forming regions in the central degree (Yusef-Zadeh, Morris & Chance, 1984)
- some compact and evolved H II regions with stars of type B0 and earlier (Liszt & Spiker, 1995).
- about $1/10^{\rm th}$ the mass and column density of Sgr B

2 Goals and analysis

We are studying Sgr B and Sgr C to

1. examine the distribution of 6.4 keV emission from fluorescent iron and reexamine ideas for its origin
2. study the relationship between prominent X-ray and radio sources in active star formation regions.

To study the origin of the 6.4 keV emission, we need to accurately map the amplitude, equivalent width, and other properties of this spectral feature. For this study, we developed a method to image spectral characteristics by extracting and fitting spectra from an array of tiles on an X-ray observation. The best fit parameters from spectral fits are then mapped back onto the sky.

While the tilemap technique loses some spatial resolution, there are several advantages:

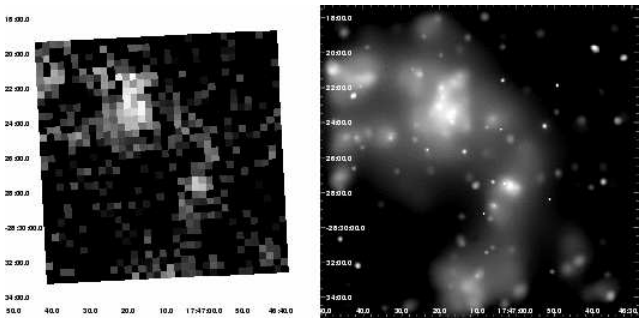

Figure 1: A comparison of our "tilemap" image on the left to an adaptively smoothed image (right) of 6.4 keV emission from Sgr B. "Sgr B2" is the name given to the northern half of the H II region, where the 6.4 keV emission is brightest; "Sgr B1" is located in the bottom center of these images.

- Each tilemap pixel value has an associated error bar, making results more robust.
- Spectral fits are less affected by continuum emission, producing a more accurate map of the line emission.
- Response files and background spectra are tailored to each region for improved accuracy.
- Any spectral parameter (e.g., absorbing column, temperature) can be mapped.

3 Sgr B and fluorescent iron

The fluorescent iron line at 6.4 keV is most commonly produced when hard X-ray photons (> 7.1 keV) knock off an iron K-shell electron. Murakami et al. (2000) have suggested the following

- the morphology of 6.4 keV emission from Sgr B suggests Sgr A* illuminated it
- Sgr A* must have been 10^6 times its present luminosity to have caused the Sgr B fluorescence
- this dramatic change in luminosity must have occurred in the last 300 years, the light travel time from Sgr A* to Sgr B.

A factor of 10^6 increase in luminosity, and the corresponding increase in mass inflow/outflow, suggests that Sgr A* could have had an active galactic nucleus like appearance. However, the unusually active star formation in Sgr B may provide another source for the required hard X-rays.

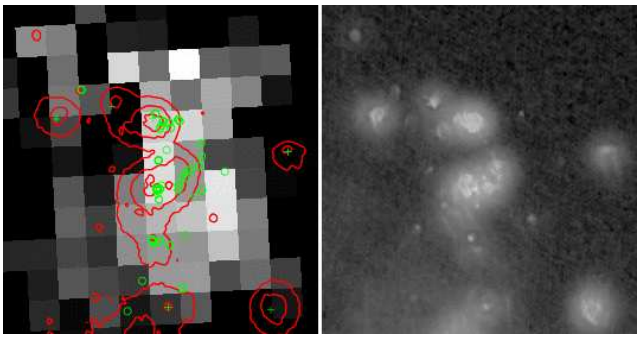

Figure 2: The left image shows a close-in view of the 6.4 keV emission from Sgr B2 (the northern portion of Sgr B) with a pixel size of 25″ (1 pc at 8.5 kpc). Contours show 20 cm radio continuum, also shown in grayscale on the right. Green circles show maser emission. The right image shows 20 cm radio continuum emission.

3.1 External versus internal irradiator

Murakami et al. (2000) calculate the required Sgr A* X-ray luminosity for the Sgr B fluorescence as

$$L_{2-10\ \mathrm{keV}} \sim 3\times10^{39} \left(\frac{d}{100\ \mathrm{pc}}\right)^2\ \mathrm{erg\ s^{-1}},$$

where d is the separation between the irradiator and Sgr B (pixel size in Fig. 1 and 2 is 1 pc).

They argue against irradiation by sources inside Sgr B based on the required luminosity and the spatial distribution of the *X-ray* sources. However,

- The high column densities toward the main part of Sgr B2 can extinguish much of the X-ray flux that may be there; we find that there could be $L_{2-10\ \mathrm{keV}} \sim 10^{34}$ erg s^{-1} hidden by the cloud.
- The 30 compact H II regions which are undetected by *Chandra* should contribute significantly to the irradiation of the cloud; each has O and B stars with $L_{2-10\ \mathrm{keV}} \sim 10^{31-32}$ erg s^{-1}.
- Since the stars in Sgr B2 are forming in ultracompact H II regions, they can irradiate the surrounding molecular material very efficiently (i.e., d, in the above equation is < 1 pc).
- The equivalent width of 6.4 keV line varies widely (from 0.5–3 keV), inconsistent with that expected for an external irradiator ($\sim$ 1 keV) (Fromerth, Melia & Leahy, 2001).
- The distribution of 6.4 keV emission is similar to the distribution of masers and H II regions (see Fig. 2).

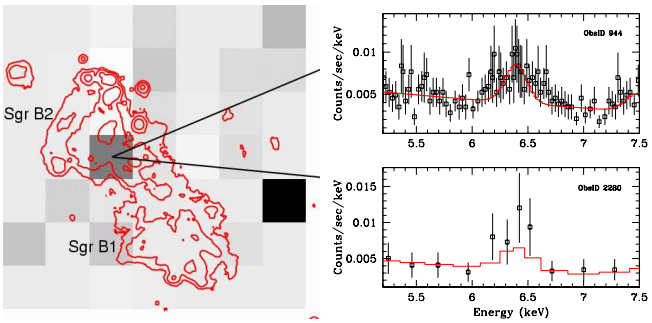

Figure 3: The left image is a 150″ (6 pc) resolution map of the estimated significance of variability in the 6.4 keV line toward Sgr B. On the right are spectra from the two observations of the region indicated in the left image. The top spectrum is from the first (longer) observation with best-fit Gaussian to the 6.4 keV line; the bottom spectrum has data points from the second observation with the same model plotted for comparison.

The idea that the fluorescence is caused by sources internal to Sgr B2 will be explored more fully in a future paper.

3.2 Variability in fluorescence

Sgr B was observed twice by *Chandra* over a 1.5 year span. We have mapped the 6.4 keV flux in the two observations of Sgr B2 and find one area where 6.4 keV flux may have increased between the two epochs. Figure 3 shows a map of the significance of variability in the 6.4 keV across Sgr B2; the spectra from the two observations of an identical region are also shown. The best-fit model to the first observation (ObsID 944) underestimates the 6.4 keV flux in the second observation (the 90% errors of the line amplitudes exclude each other). No variable point sources are in this region, nor are there any point-like sources of 6.4 keV emission. One caveat is that the ACIS chip gap crosses this region in both observations; however, the gap covers *more* of the region in the second observation, suggesting that the overall flux should decrease (instead of increase as we observe).

4 Sgr B1 point sources

Figure 4 shows the best-fit X-ray spectrum of the point sources in the Sgr B1 H II region. The high-energy line and continuum emission from the Sgr B1 point sources suggests an unusually hot thermal component (or a powerlaw one), while low-energy line emission requires a cooler thermal model. Best fit model is the

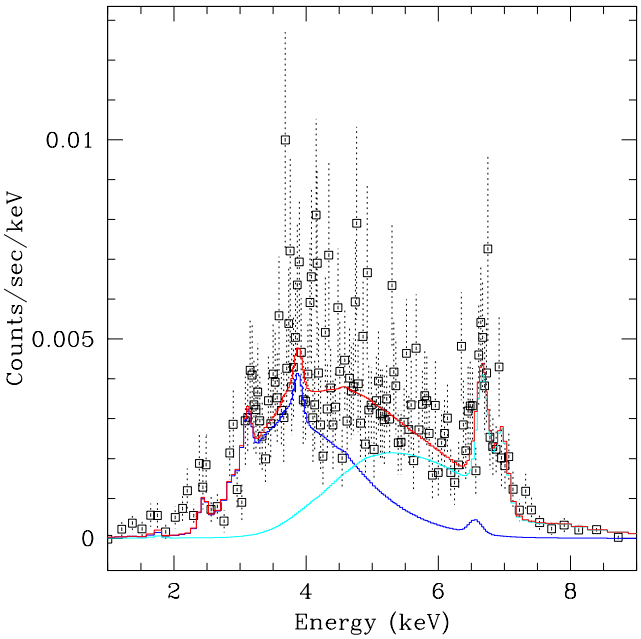

Figure 4: X-ray spectrum from the 80 sources within Sgr B1, with best-fit model in red and the two components which comprise this model in blue and cyan.

sum of these components, with values of:

- $N_{\rm H\ 1} = 23^{+6}_{-7}\times10^{22}$ cm^{-2}, $kT = 0.9^{+0.4}_{-0.3}$ keV, $L_{0.5-8\ \rm keV} = 5\times10^{34}$–$2\times10^{36}$ erg s^{-1} — highly absorbed, typical thermal emission
- $N_{\rm H\ 2} = 47^{+25}_{-56}\times10^{22}$ cm^{-2}, $kT = 9^{+9}_{-2}$ keV, $L_{0.5-8\ \rm keV} = 1\times10^{31}$–$3\times10^{34}$ erg s^{-1} — very highly absorbed, hot thermal emission

About 1/3 of these sources are variable; the variable sources have twice the count rate of the non-variable (36 versus 18 per 100 ks).

The spectrum shown in Wang, Gotthelf & Lang (2002), of the $\sim$ 1000 point sources in the *Chandra* galactic center (GC) survey is similar to what is shown in Fig. 4. The low-energy portion of the spectrum is best described by absorbed thermal emission from massive stars, while the high-energy portion shows a hot thermal ($>$ 8 keV) or non-thermal contribution.

5 Sgr C

Figure 5 and 6 compare X-ray continuum, radio continuum, and molecular line emission for the Sgr C H II region. We found two regions of interest: a diffuse X-ray continuum feature in the southeast and a peak in

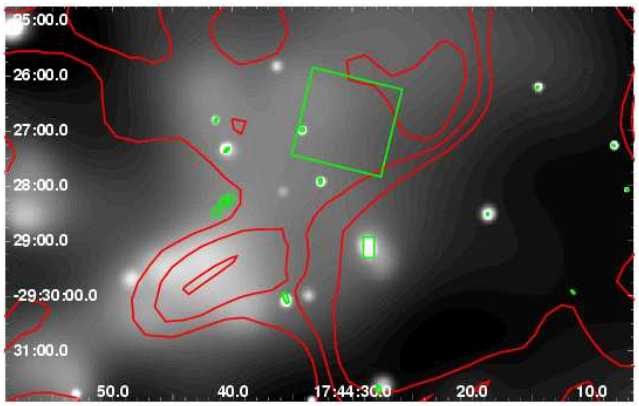

Figure 5: Grayscale shows adaptively-smoothed X-ray emission and red contours show CS (1–0) emission from -130 to -120 km s^{-1} (Tsuboi, Handa & Ukita, 1999). Ellipses show X-ray point sources, circles show maser positions, and rectangle shows a $20''$-long filament. The large square region shows the region of brightest 6.4 keV emission, as determined from a tilemap.

the 6.4 keV emission toward the northwest. Both have possible counterparts in CS (1–0) maps.

- The diffuse X-ray continuum feature has 6.4 keV emission with an equivalent width of 0.5 keV.
- Stronger 6.4 keV emission is found to the northwest with an equivalent width of ~ 1.5.
- The diffuse feature is nicely aligned with molecular CS in the -130 to -120 km s^{-1} range, far from the typical velocity of the Sgr C maser and H II emission around -50 km s^{-1} (see Fig. 5).
- Northwest 6.4 keV feature appears to be coincident with CS (1–0) emission at velocities similar to maser and H II emission, at -60 to -50 km s^{-1}.
- The position of the 6.4 keV feature is shifted east of that reported by Murakami et al. (2001), possibly because a chip gap lies in part of our map. Murakami et al. (2001) correlate their 6.4 keV feature in Sgr C with a peak in CS (1–0) at -120 to -110 km s^{-1}.

Other points of interest include:

- Small ($\sim 20''$ long) elongated X-ray feature (small rectangle in Fig. 6) is located adjacent to a thermal ridge of emission identified by Liszt & Spiker (1995).

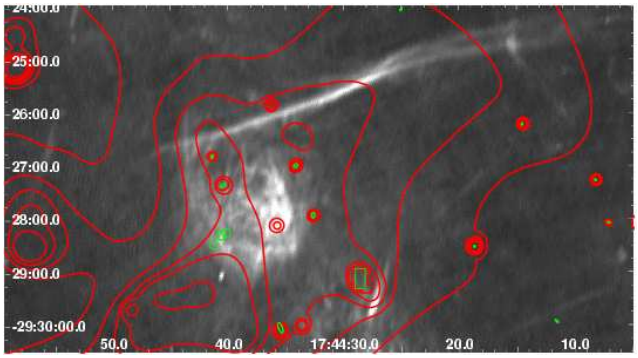

Figure 6: Radio continuum image with contours of X-ray continuum. Regions are the same as for Fig. 5.

- No X-ray emission coincident with non-thermal filament, although diffuse X-ray emission pervades the region.
- A 100-count X-ray spectrum from all sources has too few counts to show obvious line emission (e.g., highly ionized iron, at 6.7 keV). Absorption is consistent with GC location ($N_{\rm H} \sim 10^{23}$ cm^{-2}).

6 Summary and discussion

- Variability in fluorescent iron emission is tentatively detected adjacent to Sgr B2. If confirmed, this variability would be consistent with a reflection model. Variability in 6.4 keV fluorescence may be caused by Sgr A* flare propagating across Sgr B or flares from stars *inside* Sgr B.
- The current variability map is not sensitive enough to directly show propagation of 6.4 keV emission.
- Diffuse X-ray emission, particularly the 6.4 keV fluorescent iron line, is found toward Sgr B1 and Sgr B2. Fluorescent iron emission from Sgr B2 may be accounted for by irradiation by sources internal to the cloud.
- We find 80, highly-absorbed X-ray point sources throughout Sgr B1; the density of these sources is greater than those seen in Sgr B2. Sgr B1 point source spectrum is comprised of cool and highly-absorbed, hot thermal components. This is consistent with the idea that Sgr B1 has exposed and embedded stars; suggesting that star formation is still ongoing. The similarity of this spectrum with

that of all X-ray point sources in the GC region may suggest that star formation in Sgr B1 is typical for the GC.

- Sgr C has two regions of iron fluorescence with different equivalent widths (and possibly different velocities for their molecular counterparts), and may have different origins.

Acknowledgments

We acknowledge support by NASA grant NAS8-39073. This research has made use of NASA's Astrophysics Data System.

References

Fromerth, M. J., Melia, F., Leahy, D. A. 2001 ApJ, 547, L129

Liszt, H. S., Spiker, R. W. 1995, ApJS, 98, 259

Mehringer, D. M., Palmer, P., Goss, W. M., Yusef-Zadeh, F. 1993, ApJ, 412, 684

Mehringer, D. M., Menten, K. M. 1997, ApJ, 474, 346

Murakami, H., Koyama, K., Sakano, M., Tsujimoto, M., Maeda, Y. 2000, ApJ, 534, 283

Murakami, H., Koyama, K., Tsujimoto, M., Maeda, Y., Sakano, M. 2001, ApJ, 550, 297

Sato, F., Hasegawa, T., Whiteoak, J. B., Miyawaki, R. 2000, ApJ, 535, 857

Tsuboi, M., Handa, T., Ukita, N. 1999, ApJS, 120, 1

Wang, Q. D., Gotthelf, E. V., Lang, C. C. 2002, Nature, 415, 148

Yusef-Zadeh, F., Morris, M., Chance, D. 1984, Nature, 310, 557